

Original Article

Diversification over deep and shallow temporal scales in the Holarctic genus *Perpolita* (Gastropoda: Gastrodontidae)

Takumi Saito^{1,*}, Jeffrey C. Nekola¹, Markéta Nováková¹, Eva Líznarová¹, Takahiro Hirano², Veronika Horskáková¹, Michal Horskák¹

¹Department of Botany and Zoology, Faculty of Science, Masaryk University, Kotlářská 2, CZ-611 37 Brno, Czech Republic

²Biology Program, Faculty of Science, University of the Ryukyus, Nishihara-Cho, Senbaru 1, 903-0129, Okinawa, Japan

*Corresponding author. Department of Botany and Zoology, Faculty of Science, Masaryk University, Kotlářská 2, CZ-611 37 Brno, Czech Republic.

E-mail: saito.zef@gmail.com

ABSTRACT

The Holarctic land snail genus *Perpolita* was used to explore the influence of past and current biogeography on diversification. The number of empirically-supported species was determined using a consensus between mtDNA sequence, nDNA sequence, conchology, and geographic and ecological range with five valid temperate-boreal species (*Perpolita binneyana*, *Perpolita electrina*, *Perpolita hammonis*, *Perpolita petronella*, and *Perpolita radiatella*) being recognized. Only *P. petronella* was unchanged in both nomenclature and diagnostic characteristics with the remainder requiring alterations. Perhaps the most important of these was elevation of *P. radiatella* to a valid species, with its populations having been previously lumped either under European *P. hammonis* or North American *P. electrina*. Divergence times of 18.7–10.0 Mya were suggested through genome-wide SNPs in combination with the fossil record, indicating a pre-Pleistocene origin for all *Perpolita* species. Using genetically-confirmed diagnostic shell characters, we accumulated > 2000 valid occurrences and used these to estimate appropriate modern and Last Glacial Maximum climate extents for all species. These models suggest that modern intra-specific gene pool diversity may generally reflect Pleistocene palaeoclimatology.

Keywords: biogeography; ddRAD-seq; integrative revision; Last Glacial Maximum; morphology; *Nesovitrea*; taxonomic error

INTRODUCTION

Current biodiversity is not only related to modern environmental gradients, ecological interactions, and biogeography but also to the historical template (e.g. Ricklefs and Schluter 1993, Nekola and White 1999). While cyclic Pleistocene climate change has been implicated in diversification (e.g. Weir and Schluter 2004, Hope *et al.* 2012, Weir *et al.* 2016), many species' origins pre-date the Pleistocene (e.g. Toews and Irwin 2008, Kleckova *et al.* 2015, Schär *et al.* 2018). The diversification process must thus consider a mix of both ancient and recent drivers.

The land snail genus *Perpolita* H.B. Baker, 1928 appears potentially useful in considering such issues. It likely originated in the Oligocene (Schlickum and Strauch 1975), and is currently believed to represent six nominal species and one subspecies across the Holarctic (MolluscaBase 2024). While some authors have placed this genus within Hawaiian *Nesovitrea* C.M. Cooke, 1921 (e.g. Hubricht 1985, Sysoev and Schileyko 2009, Welter-Schultes 2012), this act has not been based on any

empirical tests. Hausdorf (1998), Bouchet *et al.* (2017), and MolluscaBase (2024) keep these genera separate, and we follow that approach here. Two species [*Perpolita petronella* (L. Pfeiffer, 1853), *Perpolita hammonis* (Strøm, 1765)] are thought limited to Eurasia (Sysoev and Schileyko 2009, Welter-Schultes 2012), two [*Perpolita binneyana* (E.S. Morse, 1864); *Perpolita electrina* (Gould, 1841)] to temperate/boreal North America (Pilsbry 1948, Hubricht 1985), with the remaining two [*Perpolita dalliana* (Pilsbry & Simpson, 1889), *Perpolita suzannae* (Pratt, 1978)] being limited to warm temperate/subtropical areas adjacent to the Gulf of Mexico in southeastern North America (Pilsbry 1948, Hubricht 1985). In addition, *P. binneyana* has been segregated into two subspecies with *Perpolita binneyana occidentalis* H.B. Baker, 1930 being used to demarcate populations west of 100°W (Pilsbry 1948).

This genus demonstrates parallel shell traits in species restricted to different continents, with *P. electrina*/*P. hammonis* both possessing darker shells and *P. binneyana*/*P. petronella*

Received 31 October 2023; revised 3 April 2024; accepted 21 May 2024

© 2024 The Linnean Society of London.

This is an Open Access article distributed under the terms of the Creative Commons Attribution-NonCommercial License (<https://creativecommons.org/licenses/by-nc/4.0/>), which permits non-commercial re-use, distribution, and reproduction in any medium, provided the original work is properly cited. For commercial re-use, please contact reprints@oup.com for reprints and translation rights for reprints. All other permissions can be obtained through our RightsLink service via the Permissions link on the article page on our site—for further information please contact journals.permissions@oup.com.

possessing lighter/uncoloured shells. Additionally, while the ecological niches for all four boreal taxa overlap to some extent, *P. binneyana*/*P. hammonis* both tend to occupy drier sites than *P. electrina*/*P. petronella* (Nekola 2004, Welter-Schultes 2012, Horsák *et al.* 2013). Given that empirical testing of these taxonomic hypotheses has never been attempted, it is unclear whether the patterns are real and require an evolutionary explanation, or whether they simply reflect unjustified taxonomist exuberance within phenotypically or ecologically plastic taxa (e.g. Nekola and Horsák 2022).

We investigate these issues through a global analysis of all currently recognized *Perpolita* taxa. We first determine the number of empirically supported taxa using mtDNA sequence, nDNA sequence, and shell morphology as our distinct data streams. We then use nDNA SNP data in combination with dated fossils to document species-scale diversification. We use these genetically-verified concepts to determine robust shell identification features, and then use these characters to generate valid range and occurrence information for each species. These data were used to estimate the geographic extent of modern and Last Glacial Maximum (LGM) climate niches of each species through ecological niche modelling (ENM). The impact of past and present ranges on the modern intraspecific gene pool diversity was then considered.

MATERIAL AND METHODS

Taxon sampling and DNA methods

We analysed 111 individuals representing the entire ecological and biogeographic range of all currently recognized *Perpolita* taxa. These were sourced from 22 countries and generally collected from 1995–2022 (Supporting Information, Table S1; Fig. 1). Specimen selection was undertaken through an iterative process: we initially assembled a set of 30 individuals (e.g. 3–6 per taxon) across the known geographic and ecological range of all taxa using currently accepted taxonomic concepts and diagnostic characters (Pilsbry 1948, Sysoev and Schileyko 2009, Welter-Schultes 2012, Hayase *et al.* 2016). These were subjected to an initial phylogenetic analysis, with concordance/discordance between prior and actual highly-supported concepts being noted. We then sorted material into genetically-validated groups and used these to determine potential robust diagnostic shell characters. The ability of these to accurately demarcate genetic clades was then tested by using them to select additional individuals from other populations. These then had their identifications verified using both mtDNA and nDNA sequence barcodes. This procedure was repeated until no mismatch occurred between morphological and genetic-based identifications. Documented robust traits were then used to select a final group of individuals to ensure the total specimen set included the full biogeographic and ecological extent of each genetically confirmed entity. Following selection, each specimen was imaged (see below) with total DNAs then being extracted using the E.Z.N.A. Mollusc DNA Kit (Omega BioTek, GA, USA) following manufacturer protocols.

We amplified and sequenced one mitochondrial [cytochrome *b* (Cytb)] and two nuclear regions [Internal Transcribed Spacer 1 of the rRNA gene cassette (ITS1) and Intron 8 of the

Embryonic Lethality and Abnormal Visual System (ELAV8; Nekola *et al.* 2022b)] per specimen. Primers and amplification protocols are provided in Table 1. Following ExoSAP purification of PCR products, Sanger sequencing was conducted on each by the SEQme s.r.o. laboratory (Czech Republic) using the Gerbera Sequencing Kit v.3.1. The primer ends were removed, and all resulting sequences were deposited in GenBank (accession nos PP565243–PP565334 and PP573309–PP573503).

Molecular phylogenetics

Phylogenetic analyses were independently performed on each locus to detect potential topological incongruences using MEGA 7 (Kumar *et al.* 2016). MUSCLE (Edgar 2004) was employed to align each dataset with default parameters. Final alignments were adjusted by eye. To reduce phylogenetic uncertainty, alignment gaps in ELAV8 and ITS1 were eliminated using trimAl 1.2 (Capella-Gutiérrez *et al.* 2009). Identical haplotypes were collapsed with FaBox 1.61 (Villesen 2009). Maximum likelihood analyses (ML) were conducted using IQ-TREE v.2.2.0 (Minh *et al.* 2020). PartitionFinder 2 (Lanfear *et al.* 2017) was employed to select evolutionary models and partitions based on corrected Akaike information criterion (AICc; Table 2). Ultrafast bootstrapping (Hoang *et al.* 2018) with 1000 replicates was utilized to evaluate the ML tree topologies. Bayesian inference analyses (BI) were performed using MrBayes 3.2.7a (Ronquist and Huelsenbeck 2003), with four simultaneous chains and sampling trees every 1000 generations. All datasets were run for 1 million generations with four chains. The first 101 trees were discarded as burn-in after assessing convergence with Tracer v.1.7 (Rambaut *et al.* 2018) and ensuring that the effective sample size (ESS) of all parameters in each dataset was greater than 200. The remaining trees were then used to estimate each maximum clade credibility tree and to evaluate each tree topology with Bayesian posterior probability (BPP) derived from the posterior samples using MrBayes 3.2.7a.

Because ITS1 and ELAV8 showed no topological incongruencies within highly supported branches (Supporting Information, Figs S1–S3), both were concatenated into a single nDNA construct on which the following phylogenetic analyses were based. However, because of topological inconsistencies, mtDNA and nDNA data streams were analysed separately with consensus patterns being identified.

Genome-wide Single Nucleotide Polymorphisms methods

We also performed genome-wide Single Nucleotide Polymorphism (SNPs) analysis to estimate phylogeny across a broader part of the nuclear genome. This was limited to 16 individuals spread across the five empirically validated Holarctic species-level groups identified in the above analyses with subtropical *P. dalliana* being used as the outgroup (Supporting Information, Table S1). Genome-wide SNPs were obtained through double digest restriction-site associated DNA (ddRAD) sequencing (Peterson *et al.* 2012). This method has recently been used to study a variety of non-model organisms including molluscs (e.g. Haponski *et al.* 2017, Sano *et al.* 2022, Hirano *et al.* 2023). To construct the sequencing library, a double digest was performed using two restriction enzymes (*EcoRI* and *MspI*) with approximately 50 ng of extracted genomic DNA. P1 and P2

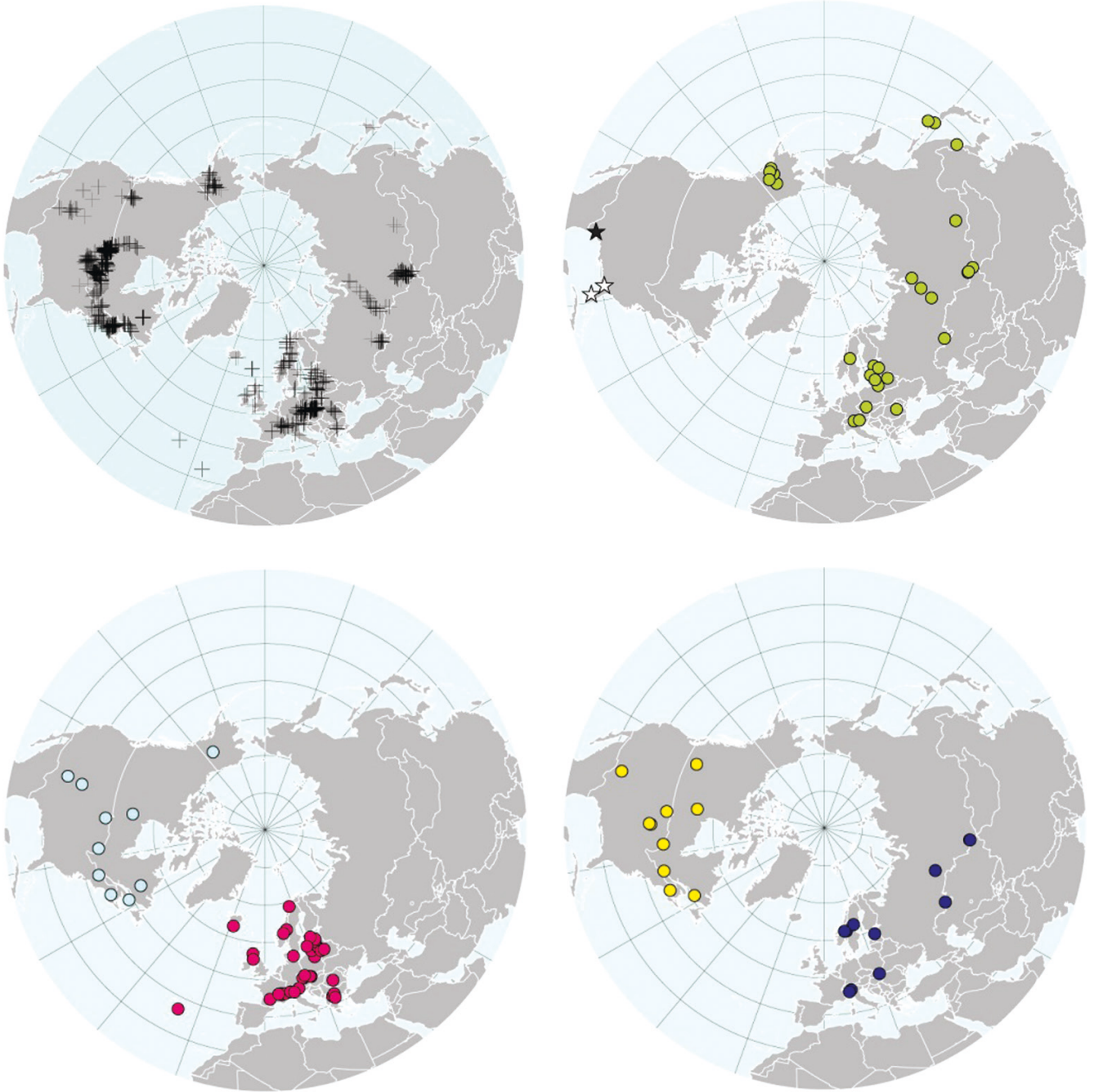
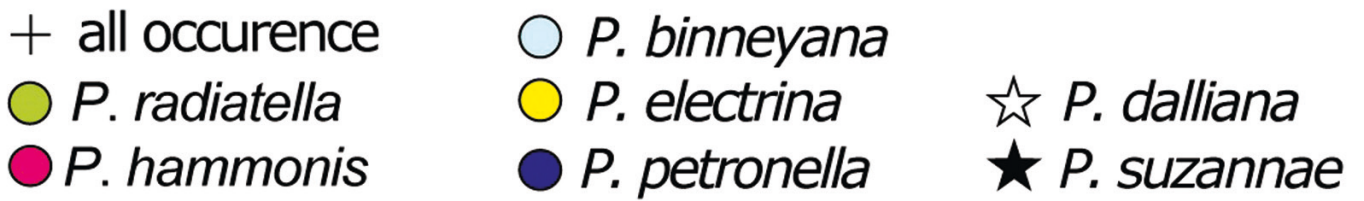


Figure 1. Distribution of *Perpolita* occurrences used in this study. The black crosses indicate all examined samples, and the coloured dots represent samples used in the molecular analyses. Map retrieved from Natural Earth (<https://www.naturalearthdata.com/>), and presented with the azimuthal equidistance projection centred on the North Pole using QGIS 3.16 (QGIS Development Team 2020).

Table 1. Information on primers and PCR conditions used in this study. See also Nekola et al. (2022b) for PCR of the ELAV8 region

Primer	Direction	Sequence 5'-3'	PCR conditions	Reference
Cytb				
CytB_Nes_fe	Forward	GGA CGT GGA AIT TAT TAT CAA AG	96 °C 10 min, (94 °C 30 s, 45 °C 30 s, 72 °C 60 s) × 40, 72 °C 10 min	Authors
CytB_NesUni_r	Reverse	GCR AAT AAR AAA TAT CAC TCR GG		Authors
ITS1				
ITS1-F	Forward	TAA CAA GGT TTC CGT ATG TGA A	96 °C 10 min, (94 °C 30 s, 52 °C 30 s, 72 °C 60 s) × 40, 72 °C 10 min	Armbruster et al. 2000
ITS1-R	Reverse	TCA CAT TAA TTC TCG CAG CTA G		Horsáková et al. 2019
ELAV8				
ELAVF_NI_100	Forward	ATG ACA CAG TTG GAC TTG GAG	96 °C 10 min, (94 °C 30 s, 52 °C 30 s, 72 °C 60 s) × 40, 72 °C 10 min	Nekola et al. 2022b
ELAVF_NI_84	Reverse	GAG AAC AAC TTC TCC AAA TCC T	(slightly modified by authors)	Nekola et al. 2022b
ELAVF_NO_88	Forward	GCT AAC TIA TAT AIT AGT GGC TTG C	96 °C 10 min, (94 °C 30 s, 50 °C 30 s, 72 °C 60 s) × 40, 72 °C 10 min	Nekola et al. 2022b

adapters from Peterson et al. (2012) were ligated to the digested DNA fragments. After the ligation, the DNA fragments were multiplexed and then purified using NucleoSpin Gel and PCR Clean-up kit (Macherey-Nagel, Germany). The library was then amplified for 10 PCR cycles. PCR conditions followed the protocol of Peterson et al. (2012), with final primer concentration being modified to 0.5 μM. Finally, the amplified sample was purified using the same clean-up kit. DNA fragments of 200–400 bp were collected using Pippin Prep (Sage Science, MA, USA). The constructed DNA library was sent to MacroGen Japan (Tokyo) and sequenced using an Illumina Hi-seq X paired-end 150 bp setting (Illumina, CA, USA). The sequenced raw reads were then processed for *de novo* assembly using ipyrad v.0.7.29 (Eaton and Overcast 2020). We specified a minimum coverage of nine (> 50%) samples per locus, with strict filter adapters (filter_adapters = 2) to completely remove the Illumina adaptor sequences. Other parameters were set to default which are adjusted by the developers in most cases. We were able to analyse 78 717 SNPs distributed across 1 171 157 bp in 4134 loci. The raw sequences were deposited in the NCBI Sequence Read Archive (PRJNA1094558).

The obtained SNPs were then used to conduct two different phylogenetic analyses: first, ML reconstruction was based on concatenated sequences using IQ-TREE v.2.2.0 (Minh et al. 2020). The nucleotide substitution model was automatically selected using ModelFinder Plus (Kalyaanamoorthy et al. 2017) as implemented in IQ-TREE (Table 2). ML tree topologies were evaluated using ultrafast bootstrapping (Hoang et al. 2018) with 1000 replicates. Second, SVDquartets (Chifman and Kubatko 2014) was implemented in PAUP * v.4.0a168 (Swofford 2002). This method estimates a tree using SNPs data under the coalescent model, unlike analysis from concatenated sequences, which may erroneously lead to high support values (Gadagkar et al. 2005), and furthermore, unlike methods using gene trees for each locus, has high statistical consistency and is considered robust against discrepancies between gene trees (Chifman and Kubatko 2014, Wascher and Kubatko 2021). All possible quartets were sampled, and the quartet Fiduccia and Mattheyses algorithm was employed for tree inference (Reaz et al. 2014). Bootstrap sampling (BS) with 1000 replications was performed to test the topology.

Divergence time estimation

We used *Perpolita wenzii* Schlickum & Strauch, 1975 from the lowermost Miocene Aquitanian period (23–20.4 Mya) in Erbach, Germany, as the oldest known *Perpolita* (Schlickum and Strauch 1975). This entity has clear *Perpolita* characters such as regular transverse striae on the upper surface, giving the shell a radiated appearance on gradually expanding coiling. We excluded the nominal oldest fossil—*Perpolita mattiaca* (O. Boettger, 1903) from the uppermost Oligocene Chattian period (23–28 Mya)—because of its wide umbilicus (1/4 of the shell width), obtusely carinated shell with lack of transverse striae, and high coil expansion rate (Boettger 1903). These characters define the shell morphology of the genus *Aegopinella* with the small size and carinated periphery making it similar to modern *Aegopinella pura* (Alder, 1830). In fact, *A. pura* was used as the comparative taxa in the original *P. mattiaca* description

Table 2. Evolutionary model and partitioning for each phylogenetic analysis based on PartitionFinder 2 estimation (Lanfear et al. 2017)

Alignment	Evolutionary model and partitioning for IQ-TREE	Evolutionary model and partitioning for MrBayes
Cytb	Cytb_pos1: TVM+G Cytb_pos2: GTR+G Cytb_pos3: F81	Cytb_pos1: GTR+G+X Cytb_pos2: GTR+G+X Cytb_pos3: HKY+X
ITS1	TVM+I+G	GTR+I+G
ELAV8	TVM+I	GTR+I
ITS1+ELAV8	ITS1: TVM+I+G ELAV8: TVM+I+G	ITS1: GTR+I+G ELAV8: GTR+I+G
ddRAD loci	K3Pu+F+I+G4	-

(Boettger 1903). The calibration was set as a lower constraint on the node of the most recent common ancestor (tMRCA) of the Holarctic *Perpolita*. The uncertainty of the upper constraint node (i.e. tMRCA for all *Perpolita*) was the reason why the lower constraint was used in the analysis. This uncertainty is due to distinct shell morphology (small size and carinated periphery) of *P. dalliana/suzannae* compared to *P. wenzi*. Therefore, we assigned *P. wenzi* to the branch before the node of the tMRCA node of Holarctic *Perpolita*. Because the phylogenetic relationship between *P. dalliana/suzannae* and the other *Perpolita* species remains uncertain (see below), the calibration was set as a lower constraint on the crown node of Holarctic *Perpolita*. We utilized a lognormal distribution with 23 Mya as the upper limit of the 95% confidence interval (CI; 23.00–16.03 Mya).

We employed two different methods to generate time-correlated trees. First we used RelTime (Tao et al. 2020) which represents a relaxed clock approach using branch lengths. This provides for computationally effective time estimation across all nodes (Tamura et al. 2012, 2018). RelTime was implemented in MEGA X (Stecher et al. 2020) using the above 95% CI and the GTR+I+G substitution model.

Second, we also used BPP 4.4.0 (Rannala and Yang 2003, Flouri et al. 2018). This estimates divergence time under a multi-species coalescent model without introgression using all SNPs loci and assuming GTR base pair substitution. A relaxed correlated molecular clock (Flouri et al. 2022) was employed, with a prior distribution of theta = inverse gamma (3, 0.002) and root tau = inverse gamma (3, 0.08) being adopted. Two hundred thousand Markov chain Monte Carlo samples were collected every two iterations after the initial 10 000 burn-in. Tracer v.1.7 confirmed that the ESS for all parameters was greater than 100. Finally, absolute divergence time with 95% CI for each node was calculated using the R package ‘bpp’ (Angelis and Dos Reis 2015, R Core Team 2022).

Comparative conchology

We recorded maximum shell width and height, umbilicus width, maximum numbers of whorls, shell colour, and strength of shell bottom grooves from 203 individuals sourced from 76 genetically validated populations across all valid species (Supporting Information, Table S1). Shells were imaged using an Olympus szx-7 microscope with an Olympus C-7070 Wide Zoom camera and QuickPHOTO MICRO software at c. 20× magnification. Images were depth composited using Combine ZM (<https://combinezm.en.lo4d.com/windows>). Microsculpture on lower shell surfaces was imaged using a Keyence vhx-5000 digital

microscope with zs-20 and zs-200 objective lenses at 200× magnification.

Climatic niche modelling

Using robust diagnostic features generated through the integrative empirical revision (see above), species identification was verified for all 1781 *Perpolita* lots in the author’s collections. As *P. radiatella* is absent from the United Kingdom, we assume that all *P. hammonis* records provided by Kerney (1999) to be correctly assigned. However, the co-occurrence of *P. hammonis* and *P. radiatella* in Sweden prevented the use of *P. hammonis* records from Waldén (2007).

These validated modern observations were then used to parameterize ENMs using protocols described in Nekola et al. (2022a). Climate data at 2.5-minute resolution was retrieved for each occurrence using WorldClim v.2 (Fick and Hijmans 2017). To avoid excessive multicollinearity, climate data was limited to seven variables relevant for land snail distribution (Bio3 = isothermality; Bio4 = temperature seasonality; Bio5 = maximum temperature of warmest month; Bio6 = minimum temperature of coldest month; Bio12 = annual precipitation; Bio15 = precipitation seasonality; Bio18 = precipitation of warmest quarter). Records were pruned to remove redundant observations until the smallest average pairwise distance in reduced PCA space was 0.05 standard deviations. The following data were used for modelling (total recorded/pruned records): *P. binneyana* = 452/180, *P. electrina* = 453/173, *P. petronella* = 280/135, *P. hammonis* = 348/203, and *P. radiatella* = 248/147 (detailed coordinates provided in Supporting Information, Table S2).

Climatic niches were generated for each species based on the protocols outlined in Nekola et al. (2022a), using the Maxent algorithm implemented in ‘maxent.jar’ (Hijmans et al. 2021) for the algorithm of ‘ENMevaluate’ function on ENMeval 2.0 (Kass et al. 2021). Maxent is a well-developed method for performing ENM without absence data (Phillips et al. 2006, 2017) and is widely used in species distribution modelling, with practical instructions (e.g. Warren and Seifert 2011, Merow et al. 2013). It is generally considered to have high accuracy (Kaky et al. 2020, Perkins-Taylor and Frey 2020, Ahmadi et al. 2023) and is particularly robust to sampling bias, which is common in field data (Ahmadi et al. 2023). Random 4-fold partitioning was used for cross-validation. As there is no absolute criterion for model selection we used area under the curve values (AUC; Lobo et al. 2008) and AICc (Warren and Seifert 2011). The best-fitting model for each species (Table 3) was then used to estimate

Table 3. Selected best models for each species in ecological niche modelling. The meaning of each letter in the feature class (FC) is as follows: L = linear, Q = quadratic, P = product, T = threshold. Regularization multipliers (RM) from one to eight were considered. See also Supporting Information (Table S4) for full information on all models

Species	Best AUC model	Average AUC	Best AICc model	AICc
<i>P. binneyana</i>	FC: LQPT/RM: 1	0.907543365	FC: LPT/RM: 2	4800.67003
<i>P. electrina</i>	FC: LQPT/RM: 1	0.933310521	FC: LQT/RM: 2	4432.596038
<i>P. radiatella</i>	FC: LQP/RM: 1	0.881006354	FC: LQPT/RM: 2	4130.013133
<i>P. hammonis</i>	FC: PT/RM: 1	0.96346953	FC: PT/RM: 2	5014.046584
<i>P. petronella</i>	FC: QPT/RM: 1	0.924949036	FC: LQT/RM: 2	3637.574817

potential range in current and LGM landscapes using dismo 1.3-9 in R (Hijmans et al. 2021). LGM climate data was predicted based on Community Climate System Model 4 (CCSM4; Gent et al. 2011), MIROC-ESM (MR; Watanabe et al. 2011), and MPI-ESM-P (ME; Jungclaus et al. 2011), and were retrieved from WorldClim v.1.4 (Hijmans et al. 2005).

RESULTS

Molecular phylogenetics

With full support all phylogenies showed that North American Gulf Coast *P. dalliana* and *P. suzannae* are highly distinct from the remaining higher-latitude *Perpolita* species (Figs 2–3; Supporting Information, Figs S1–S3). However, they possess very small intra-taxon divergence in both their mtDNA and nDNA sequence. Because they appear to represent a distantly-related evolutionary lineage, we limit the bulk of the following analyses to the remaining temperate-boreal *Perpolita* taxa.

The mitochondrial Cytb phylogeny reveals the presence of three well-supported monophylyes (UFB > 95/BPP = 1.00; *P. binneyana*, *P. electrina*, and *P. petronella*), and one partially supported monophyly (96/0.52; *P. hammonis*; Fig. 2; Supporting Information, Fig. S3). *Perpolita binneyana occidentalis* did not exist as even a poorly defined subclade within *P. binneyana* (Fig. 2; Supporting Information, Fig. S3). The lower support for *P. hammonis* is at least partially due to the presence of two intra-specific subclades, with subclade A being well supported (96/1.00) and ranging across Eurasia west of the Urals, and with subclade B being partially supported (98/0.72) and restricted to the Alps except for one haplotype from the Czech Republic (Fig. 2; Supporting Information, Fig. S3).

The largest discrepancy between prior taxonomic concepts and mtDNA sequence was observed in the highly supported species-level monophyly (100/1.00) that had been previously subsumed either into *P. hammonis* in Eurasia or *P. electrina* in Alaska. Based on the nomenclatural record—and a cursory examination of potential types—we suspect that *Perpolita radiatella* (Reinhardt, 1877) is the earliest available *nomen* for this entity, and we will use it to demarcate this clade throughout the rest of the paper. This entity is again divided into two subgroups, with subclade A (95/1.00) ranging from central and northern Europe to central Siberia, and subclade B (75/0.76) ranging from central Siberia to Alaska (Fig. 2; Supporting Information, Fig. S2). These subclades co-occur within the Altai Mountains of south-central Siberia.

The concatenated ITS1+ELAV8 phylogeny basically replicates the mtDNA topology (Fig. 2; Supporting Information,

Fig. S3) with *P. dalliana* representing a very long branch separated from the remaining Holarctic species. *Perpolita binneyana*, *P. electrina*, *P. petronella*, and *P. radiatella* formed maximally-supported monophylyes (100/1.0). Again, subclade structure in *P. binneyana* was not geographically correlated, while *P. radiatella* possessed a strongly supported (99/1.00) geographically restricted subclade ranging west of the Urals. *Perpolita hammonis* again demonstrated considerable within-clade diversity, with a highly-supported (100/1.0) Alpine subclade again being present.

The ddRAD phylogeny demonstrated a very similar topology but with much greater node support and resolution. Again, *P. dalliana* existed as a very long branch greatly removed from the remaining species. Within the Holarctic species, *P. binneyana*, *P. electrina*, *P. hammonis*, and *P. radiatella* each represented a distinct, maximally-supported (100/1.0) monophyly. While the use of only a single individual of *P. petronella* prevented species-scale clade resolution, its branch length was similar to other species. *Perpolita hammonis* was found to exist as two fully-supported (100/1.00) subclades, one ranging across Europe and the other being restricted to the Alps. *Perpolita radiatella* from central Siberia to Alaska again was found to exist in a separate subclade (100/1.00) from European populations. Again, the basal node for Holarctic taxa demarcated *P. radiatella* from the remaining species.

Divergence time

RelTime analysis (Fig. 4) suggested divergence times ranging from 18.7 Mya for *P. radiatella* (note that this is also the calibration node) to 13.4 Mya for *P. electrina*, 11.0 Mya for *P. binneyana*, and 10.0 Mya for *P. petronella* and *P. hammonis*. The divergence time between eastern and western subclades of *P. radiatella* was estimated at 4.4 Mya and between Alpine and pan-European *P. hammonis* subclades at 4.0 Mya. BPP analysis generated similar species divergence time estimates of 17.5, 13.4, 10.2, and 10.0 Mya, respectively.

Shell morphology

We found diagnostic shell differences to exist between all genetically-supported Holarctic *Perpolita* species (Table 4; Fig. 5). The development of sillons (parallel spiral grooves cut into the shell) on the lower surface (Fig. 6; Supporting Information, Fig. S4), especially near the umbilicus, represents a previously unrecognized diagnostic trait. *Perpolita binneyana* is distinguished by its pale shell colour, low spire, wide umbilicus, and absent sillons. *Perpolita petronella* also has a pale shell, but it possesses a high spire, narrow umbilicus, lower whorl expansion rate, and

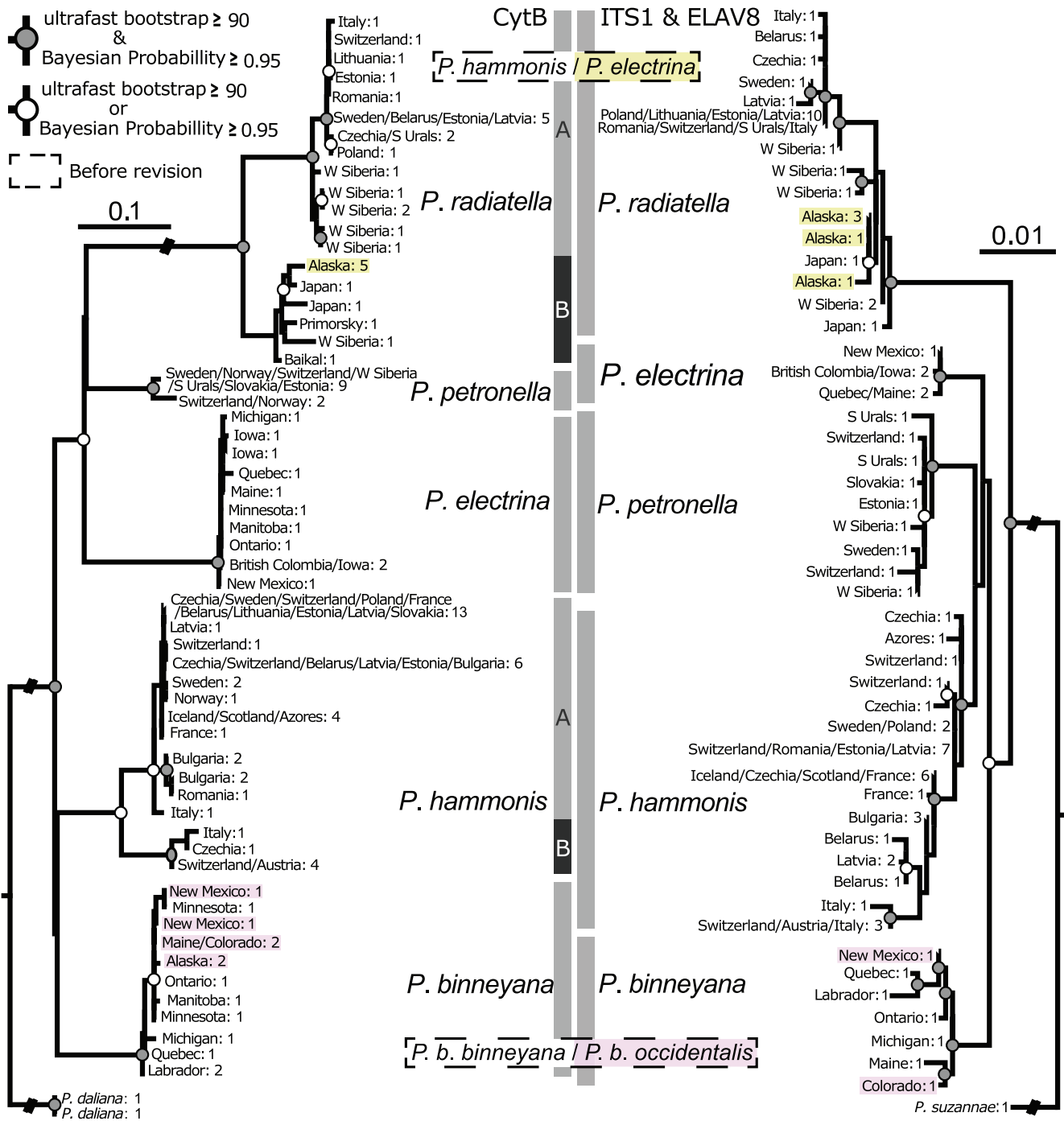


Figure 2. Maximum likelihood phylogenies of the genus *Perpolita* inferred from mitochondrial cytochrome *b*, and two nuclear regions [i.e. Internal Transcribed Spacer 1 of the rRNA gene cassette (ITS1) and Intron 8 of the Embryonic Lethality and Abnormal Visual System]. The white and grey circles on each node indicate the level of support values in ultrafast bootstrapping and Bayesian posterior probability. The labels at the branch tips indicate the number of collapsed sequences and the region in which they were sampled. The species names in the dashed boxes indicate the original species name before the revision if different from the name after revision. Detailed information on each sample and 95% CI can be found in the Supporting Information (Table S1; Fig. S3).

weak sillons. *Perpolita hammonis* has the darkest shell colour of all species, as well as a wide umbilicus, more rapid whorl expansion, and strong sillons. The neotype for this taxa (Oslo Museum D27826) was found to possess all of these features, except paler colour via shell aging. *Perpolita electrina* has a lighter brown shell colour with a narrower umbilicus, a larger shell with a lower

whorl expansion rate, and missing/weak sillons. It also has the widest apertural opening of all species. *Perpolita radiatella* has a light brown shell with a low spire, moderately wide umbilicus, rapid whorl expansion rate, and weak/missing sillons. It can be distinguished from *P. hammonis* by much weaker sillons and somewhat lighter shell colour, and from *P. electrina* by its more

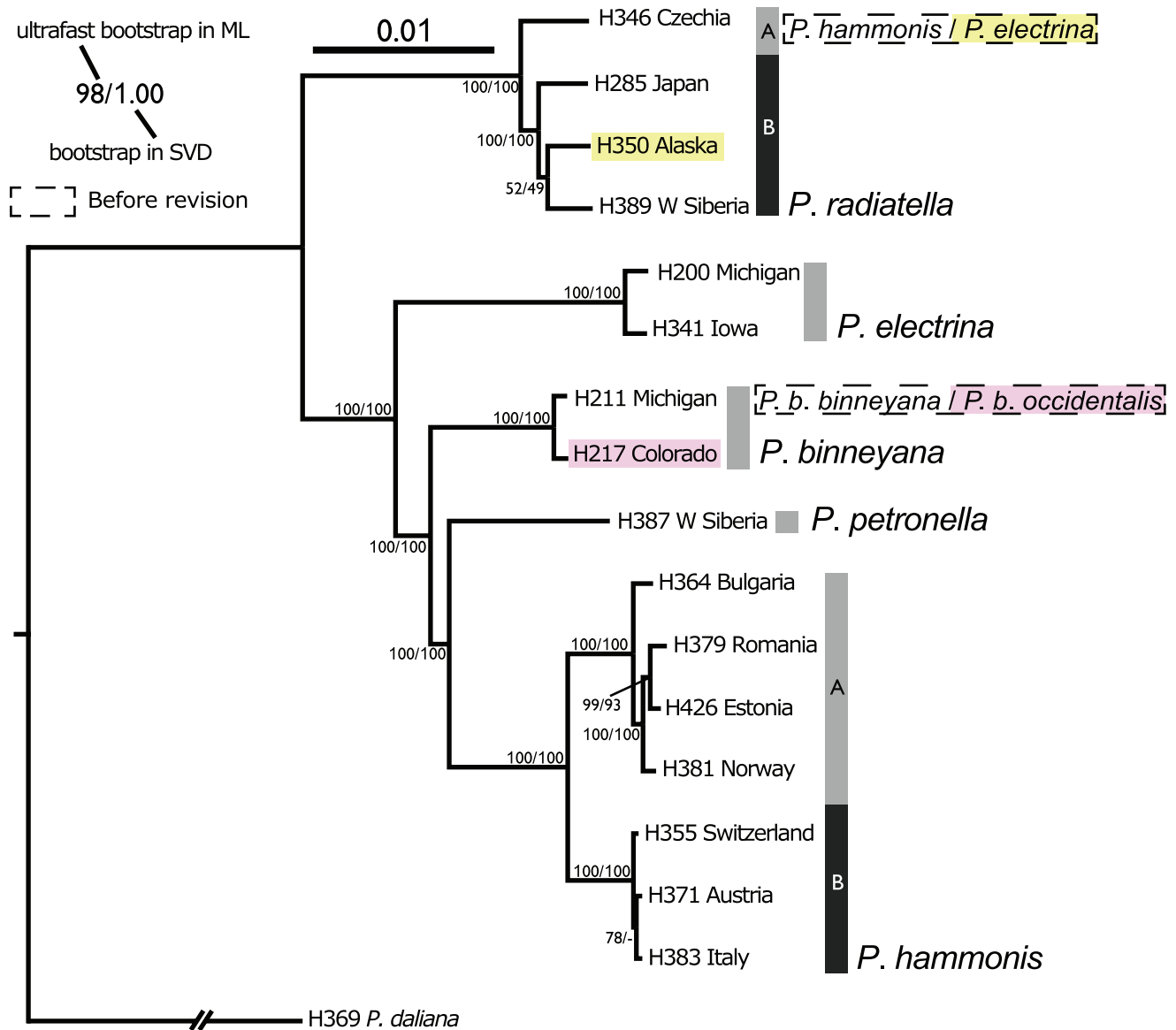


Figure 3. Maximum likelihood phylogeny of the genus *Perpolita* inferred from 1 171 157 bp that was obtained from ddRAD-seq. The species names in the dashed boxes indicate the original species name before the revision if different from the name after revision. Detailed information on each sample and 95% CI can be found in Supporting Information, Table S1.

open umbilicus, smaller median shell size, and greater whorl expansion rate.

Geographic and ecological range

Each validated species also exhibits a unique geographical and ecological range (Fig. 7). *Perpolita hammonis* extends from the North Atlantic east to the Urals, and tends to favour moderately humid and neutral-acidic forests but also occurs across a range of wooded and open wetland habitats (Welter-Schultes 2012). *Perpolita petronella* extends from the Atlantic to Altai Mountains, and appears to favour cooler and more humid sites than *P. hammonis*, particularly in Europe. *Perpolita binneyana* extends across the North American taiga from Newfoundland and Labrador to Alaska, south to the Ohio River and down the Rocky Mountains to Arizona, New Mexico, and Texas. It tends

to favour upland forest sites. *Perpolita electrina* ranges in North America from the central and north Atlantic west to the Pacific and north into the taiga, although it appears to be absent from the Beringian parts of Alaska and the Yukon. It is much more of a wetland species than *P. binneyana*, and is characteristic of fens, marshes, and nutrient-rich wet forests. Both it and *P. binneyana* are commonly sympatric in wet-mesic taiga. *Perpolita radiatella* ranges from the Atlantic coast of Scandinavia and central Europe east to Alaska. While sharing a similar environmental niche with *P. hammonis*, towards the west it tends to be limited to moister sites while it becomes more of an upland forest species in the far east.

Habitats supporting sympatric *Perpolita* (Supporting Information, Table S2) occur throughout the Holarctic and include Scandinavian and eastern European mires and humid

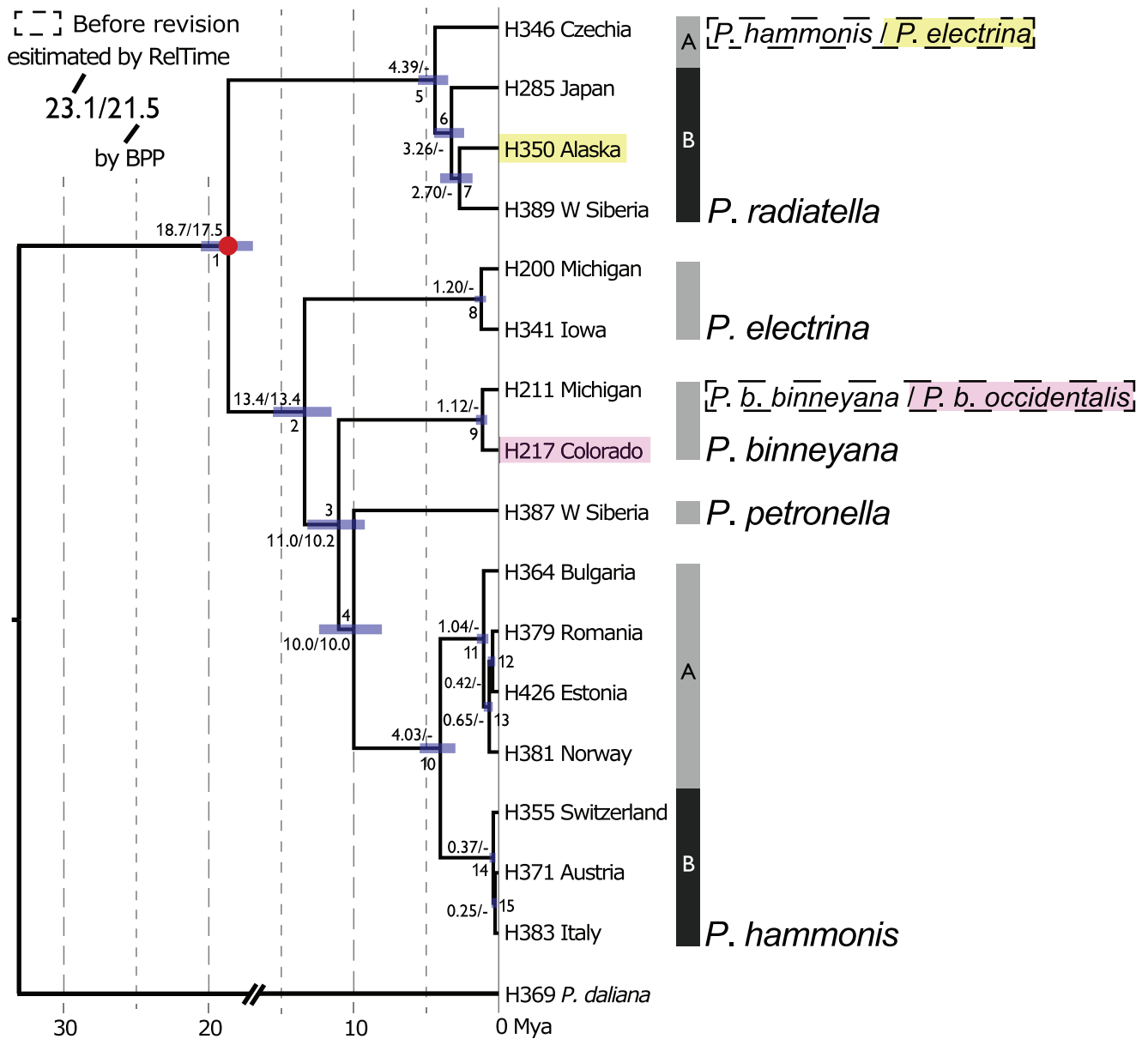


Figure 4. Divergence time estimation of the genus *Perpolita* on the maximum likelihood tree. The red circle indicates the node calibrated by the oldest known *Perpolita* fossil, and the integer number by the node referred to the node number. The blue bars at each node indicate 95% CI estimated with RelTime. The species names in the dashed boxes indicate the original species name before the revision if different from the name after revision. Detailed information on each sample and 95% CI can be found in Supporting Information (Tables S1, S3).

forests (*P. radiatella*/*P. hammonis*—nine sites, *P. radiatella*/*P. petronella*—61, *P. hammonis*/*P. petronella*—21, *P. radiatella*/*P. hammonis*/*P. petronella*—nine), central Asian hemi-boreal taiga (*P. radiatella*/*P. petronella*—52 sites), and North American cool-temperate forests and taiga from Labrador to Alaska south to Maine, Iowa, and British Columbia (*P. binneyana*/*P. electrina*—186; *P. binneyana*/*P. radiatella*—two).

Ecological niche modelling

The best Maxent climatic models based on AUC were also the highest-ranking models based on AICc (Table 3; Supporting Information, Table S4). Across all five species and all three climatic circulation models, the estimated appropriate climate

area during the LGM was smaller than in the modern era (Fig. 7; Supporting Information, Figs S5, S6). While *Perpolita hammonis* was isolated to discrete areas northwest and southeast of the Alps and to the northwest coast of continental Europe; *P. petronella* had a large and more uniform suitable climate region centred in central Europe between the Fennoscandian/British and Alpine ice sheets; *P. binneyana* and *P. electrina* existed as overlapping uniform potential distributions both ranging across southeastern North America from the Ozark Mountains to the Carolinas; *P. radiatella* occurred in approximately three isolated appropriate climate areas, one centred on Europe, one east of the Tibetan Plateau, and the other in southern Alaska. While an appropriate climate for *P. radiatella* also occurred south of the

Table 4. *Perpolita* species shell characters (following molecular revision). See also Figures 5–6 and Supporting Information, Figure S4

Species	Median width and range (mm)	Median height and range (mm)	Colour	Sillons	Spire	Aperture	Umbilicus	Maximum numbers of whorls	Whorl expansion rate (median)
<i>P. binneyana</i>	3.3 (2.8–3.9)	1.7 (1.4–2.0)	Pale ivory	Missing	Low-high	Open	Widely open	3.50	2.0
<i>P. electrina</i>	3.6 (3.2–4.2)	2.0 (1.7–2.2)	Light brown	Missing-weak	Low-high	Widely open	Narrow	3.35	1.9
<i>P. hammonis</i>	3.3 (2.9–4.4)	1.7 (1.4–2.2)	Dark brown	Strong	Low	Open	Widely open	3.55	2.2
<i>P. petronella</i>	3.9 (3.2–4.7)	2.1 (1.7–2.7)	Pale ivory	Weak	High	Open	Narrow	3.70	1.8
<i>P. radiatella</i>	3.3 (2.8–4.1)	1.7 (1.5–2.2)	Light brown	Missing-weak	Low	Open	Open	3.35	2.2

North American ice sheet, based on modern phylogeography and fossil records it appears this region was never occupied (Fig. 7; Supporting Information, Figs S5, S6).

DISCUSSION

Species diversity in *Perpolita*

Because the North American Gulf Coast *P. dalliana* and *P. suzanna* were found to occupy a distinct very long branch across mtDNA, nDNA, and SNP data, it seems likely they reside within a different sister genus. Because our data shows that these two taxa possess almost identical DNA sequences it seems likely that they are best considered a single species. Based on overall shell appearance and biogeographical range, '*Helix*' *subhyalina* L. Pfeiffer, 1867 of southeastern Mexico is likely to be part of the same group with '*P. dalliana*'. '*Glyphyalus*' *quillensis* de Winter, van Leeuwen & Hovestadt, 2016, from the Dutch Caribbean island of St. Eustatius, possesses not only a very similar shell, but 95% similarity in the CO1 sequence to *P. daliana* (De Winter et al. 2016). Given that true *Glyphyalina* (*Glyphyalus*) from the southeast USA is genetically very distinct (J. Slapcinsky, personal communication) it is clear that '*G. quillensis*' is part of the same genus-level group as '*P. dalliana*'. This putative new sister genus to *Perpolita* thus appears likely to range across the central and southern Gulf coast to at least the eastern Caribbean.

Our phylogenetic analyses of the remainder of *Perpolita* within the temperate/boreal Holarctic consistently show existence of five distinct species-level clades: *P. binneyana*, *P. electrina*, *P. hammonis*, *P. petronella*, and *P. radiatella*. Because each possesses a unique suite of conchological traits, geographic ranges, and ecological extents (Table 4; Figs 5–6; Supporting Information, Fig. S4) they can be accurately identified in the absence of molecular data. Only *P. petronella* fully followed traditional taxonomic concepts and diagnostic features (e.g. Welter-Schultes 2012, Horsák et al. 2013). In the remaining taxa significant errors existed between traditional concepts and empirical genetic data. While *P. binneyana* was confirmed as a valid species, we found no evidence of gene pool partitioning between eastern and western North American populations. We thus recommend that subspecies distinctions (e.g. *P. b. occidentalis*) be avoided. *Perpolita electrina* was found to possess a narrower range than previously thought, being limited from the Atlantic Ocean to British Columbia. Material west from the Yukon actually represented *P. radiatella*. *Perpolita hammonis* was found to possess a much more restricted range than traditionally understood, being limited from the North Atlantic (west to Iceland and the Azores) to eastern Europe. All samples initially identified as *P. hammonis* from the southern Urals eastward, as well as considerable material extending west to Scandinavia and central Europe, actually represents *P. radiatella*.

As has been previously seen (Nekola and Horsák 2022), errors in traditional taxonomic concepts represent a mix of over splitting, over lumping, and incorrect designation of diagnostic features. These can lead to significant bias in apparent ecological and biogeographic pattern. The existence of these issues within *Perpolita* is a reminder that traditional taxonomic concepts must be considered untested hypotheses requiring empirical confrontation before being accepted and used in ecological, biogeographic, and biodiversity analyses (e.g. Nekola et al. 2015,

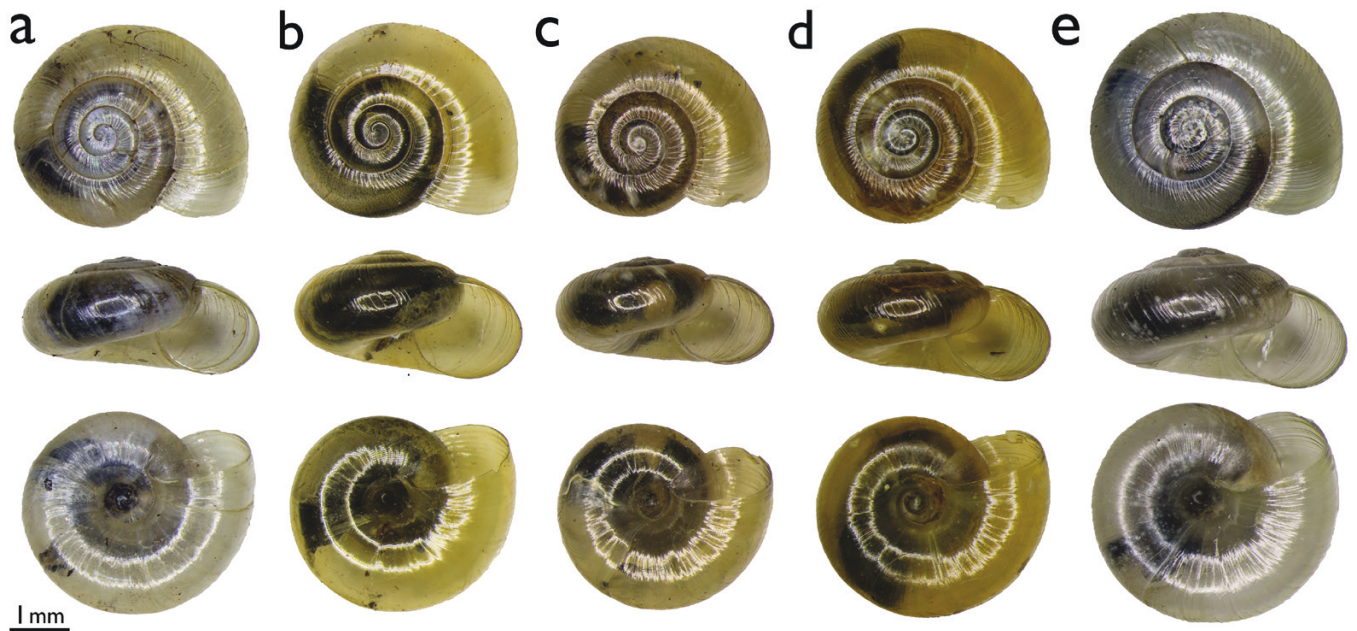


Figure 5. Shell images of each *Perpolita* species from genetically validated populations (see Supporting Information, [Table S1](#) for location details defined by sample code): (a) *P. binneyana* (H216_1; Alaska), (b) *P. electrina* (H207_1; Main), (c) *P. radiatella* (H284_1; Japan), (d) *P. hammonis* (H382_1; France), (e) *P. petronella* (H040_1; Altai Republic).

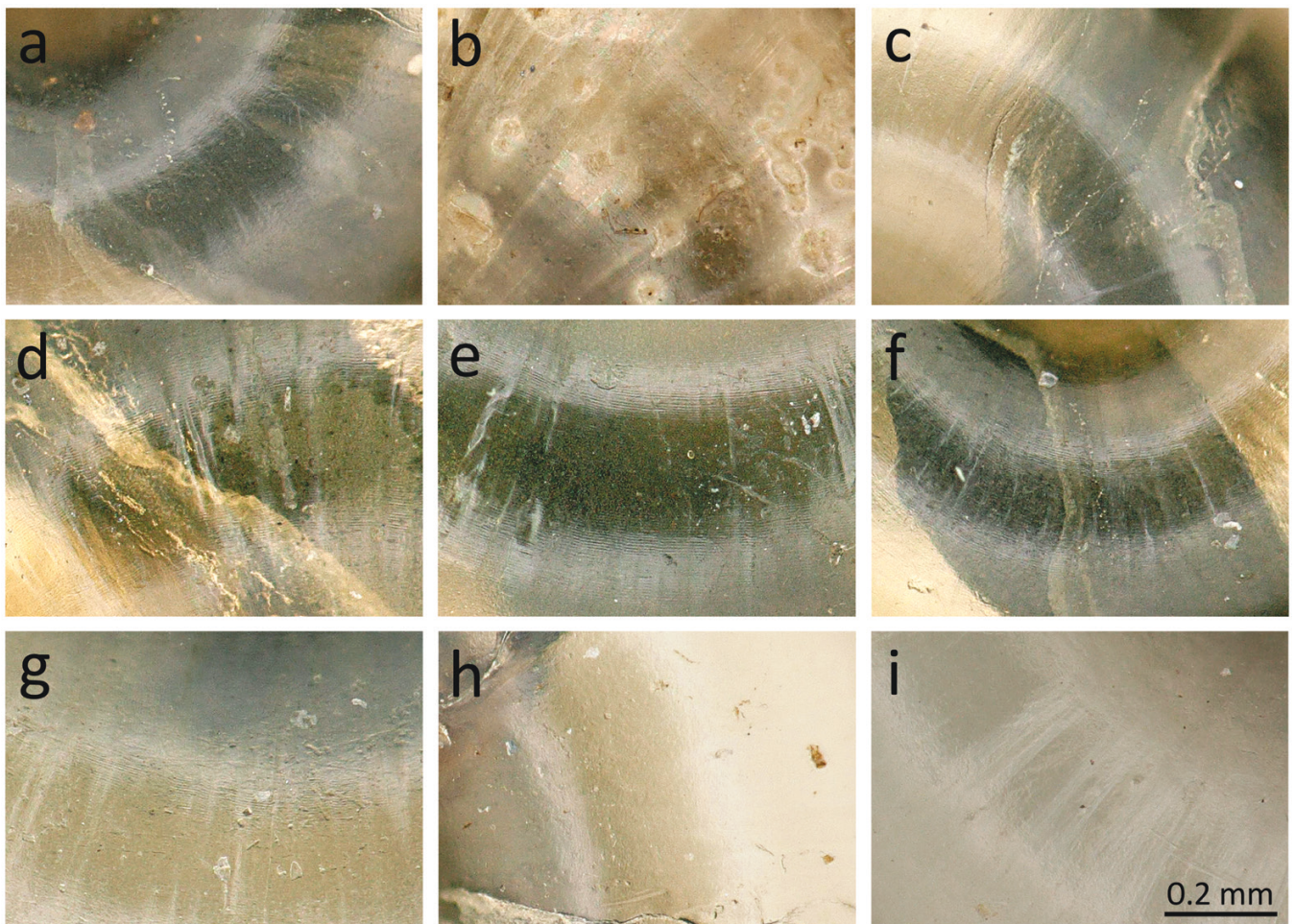


Figure 6. Development of shell bottom sillons: (a–c) *P. radiatella*; (a) H390, Belarus; (b) H340, Alaska; (c) H346, Czechia; (d–f) *P. hammonis*; (d) H046, Switzerland; (e) H382, France; (f) H432, Latvia; (g) *P. petronella*, H038, Norway; (h) *P. electrina*, H207, Ontario; (i) *P. binneyana*, H216, Alaska. See Supporting Information, [Figure S4](#) for detail of *P. radiatella* and *P. hammonis* shell bottom microsculpture.

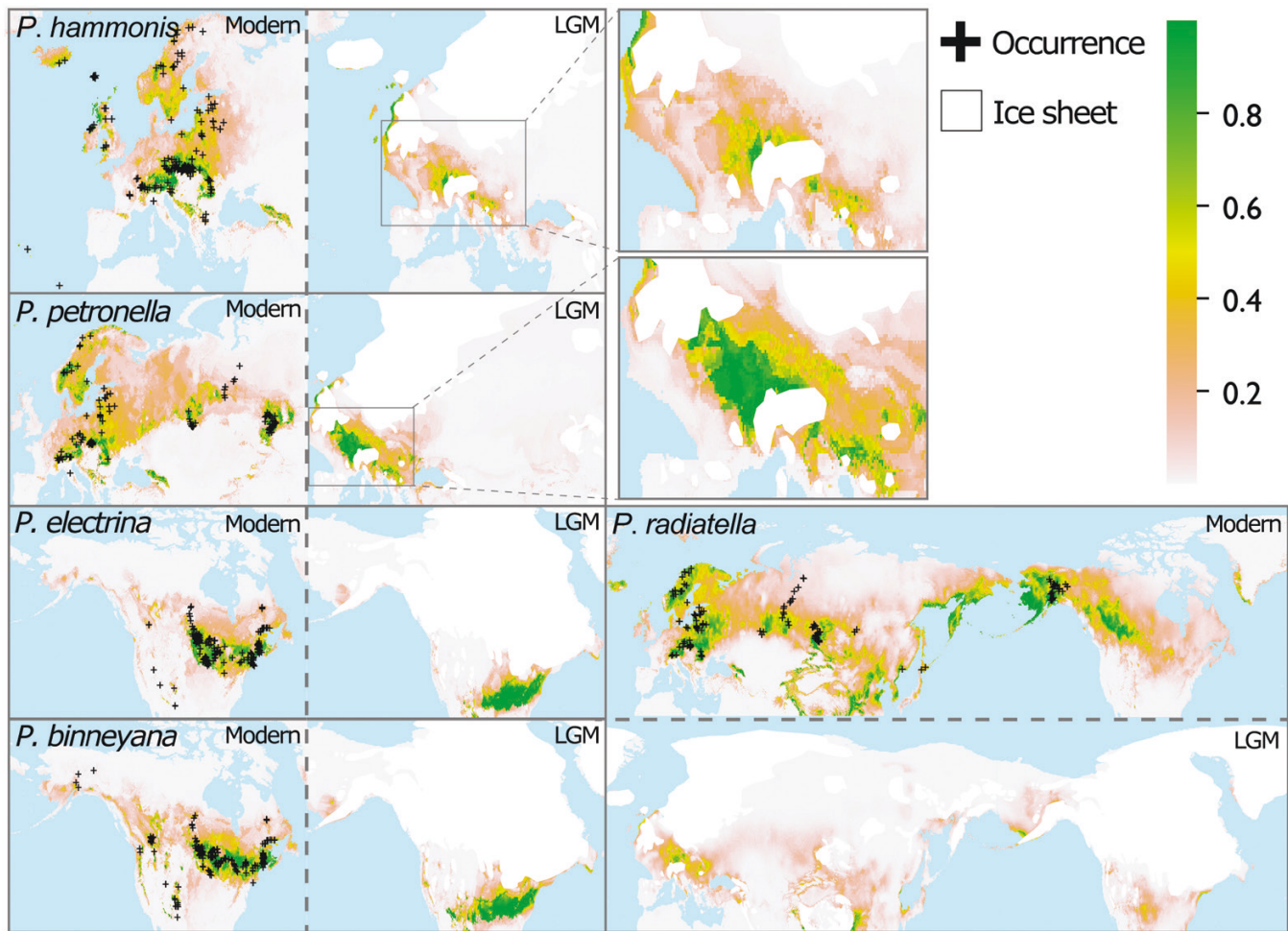


Figure 7. Potential distribution probability of each *Perpolita* species estimated by ecological niche modelling using 1.3-9 in R (Hijmans et al. 2021). The best models for each species, selected by the area under the curve based on cross-validation were used for the estimates. Occurrences on the map are environmentally pruned samples for modelling. The estimated ice sheets at the LGM are based on Ehlers et al. (2011) and the LGM climate is based on CCSM4.

2018, Aksenova et al. 2017, Horsáková et al. 2020, Bepalaya et al. 2023).

What makes this case remarkable is that *P. radiatella* was overlumped into not one but two separate taxa. The ultimate cause for this is related to the distribution of 18th and 19th century taxonomic schools whose ranges were formed when workers had limited access to information from distant areas (Graf 2007, Vinarski 2018). Thus, members of the European School overlumped Eurasian populations of *P. radiatella* into the European *P. hammonis* while those in the North American School overlumped Alaska/Yukon *P. radiatella* populations into North American *P. electrina*. This led to the generation of a perceived and artificially abrupt biogeographic transition between the North American and Eurasian *Perpolita* faunas centred on the Bering Strait. In fact, this transition is gradual and spread across the whole of Beringia. Similar spatially-autocorrelated taxonomic error has also been observed in freshwater mollusc faunas between the Russian and Western European schools (Korniushin 1998, Graf 2007, Vinarski and Kramarenko 2015, Vinarski 2018).

Unlike many other land snail genera (e.g. *Ainohelix* and *Ezohelix*: Morii et al. 2015, *Bradybaena*: Hirano et al. 2019,

Euconulus: Horsáková et al. 2019, *Pupilla*: Nekola et al. 2015, Haase et al. 2021; *Schileykula*: Harl et al. 2020) we observed no topological incongruence in individual clade membership between mtDNA and nDNA data streams. SNP-based divergence times between the five *Perpolita* species were estimated to be more than 10 Mya. While this is older than many other land snail genera (e.g. Köhler and Criscione 2014, Hirano et al. 2019, Brozzo et al. 2020, Hwang et al. 2021, Neiber et al. 2021), most of these other taxa are limited to isolated oceanic or edaphic islands. The few studies conducted on land snails possessing continental distributions demonstrate divergence times closer to our estimates (Hausdorf and Neiber 2022, Neiber et al. 2022). Thus, our evidence suggests that even though *Perpolita* species reside within northern areas greatly impacted by cyclic Pleistocene glaciations (Murray-Wallace 2023), this dynamism is likely not responsible for species-scale diversification and cladogenesis. Additionally, distribution of similar shell colours and habitat requirements across the phylograms suggests that intercontinental species pairs sharing these traits may have independently evolved these features, and that they do not represent ancestral traits.

Intraspecific diversity in *Perpolita*

Considerable variation in intraspecific gene pool size was noted between the five *Perpolita* species, ranging from little in *P. binneyana*, *P. electrina*, and *P. petronella*, to two principal subclades (likely representing separate subspecies) in *P. radiatella*, to a complex multi-clade structure in *P. hammonis*. Modern range size was a poor predictor with smallest modern range taxa (*P. hammonis*) possessing the most complex gene pool.

However, climate modelling of potential LGM distributions appears to explain these levels. Species which were predicted to possess large continuous LGM ranges (*P. binneyana*, *P. electrina*, *P. petronella*) lack clear geographic structuring in their modern gene pools. *Perpolita radiatella* possesses two well-supported intraspecific clades, one currently ranging from central Europe to central Asia, and the other from central Asia to Alaska. Both coexist within the Altai Mountains of south-central Siberia. Projected LGM distribution for *P. radiatella* suggests a highly disjunct distribution, with distributional centres located in central-east Europe and eastern Beringia. It is interesting to note that similar European vs. Beringian subpopulations have been reported (Nekola *et al.* 2015, Horsáková *et al.* 2018) in the land snails *Pupilla alpicola* and *Euconulus alderi*, with the latter harbouring disjunct European vs. Beringian projected LGM ranges (Nekola *et al.* unpubl. data).

In spite of its possession of the most limited modern range of all *Perpolita* species, *P. hammonis* demonstrated the most complex intraspecific gene structure: not only are there two well-supported subclades (one ranging across the entire species range and the other being limited to the Alps) but there are a number of additional more poorly-supported apparently spatially-restricted groups as well. LGM range reconstructions suggest its occurrences were fragmented into multiple centres of occurrence ranging from the North Atlantic coast to the west, south, and east of the Alps. The positive relationship between LGM refugia number and modern gene pool size has been previously noted in other taxa groups (e.g. Cheddadi *et al.* 2006, Dussex *et al.* 2014, Roberts and Hamann 2015). These results suggest that LGM climate change may underlie levels of subspecific diversification in *Perpolita*.

SUPPORTING INFORMATION

Supplementary data is available at *Zoological Journal of the Linnean Society* online.

ACKNOWLEDGEMENTS

We are grateful to Stefan Meng for providing the materials of *Perpolita* from eastern Siberia. We also thank Yasuto Ishii, Satoshi Chiba, Shu Nishida, and Isao Sano for supporting the ddRAD work, and Jan Divíšek for advice on ENM methods.

AUTHOR CONTRIBUTIONS

M.H., J.C.N., and V.H. collected the samples; M.H. and J.C.N. conceive the idea; T.S., M.N., E.L., and T.H. conducted the molecular work with partial support of V.H.; T.S. analysed the data and led the writing with the support of J.C.N. and M.H.; all authors reviewed and approved the final version of the manuscript.

CONFLICT OF INTEREST

None declared.

FUNDING

The study was financially supported by the Czech Science Foundation (22-230055) and the dd-RAD work was financially supported by the Japan Society for the Promotion of Science (JSPS), Grants-in-Aid for Scientific Research (KAKENHI: 23K14261), and the Showa Seitoku Memorial Foundation (Reiwa-4).

ETHICS AND PERMITS

All research pertaining to this article did not require any research permits.

DATA AVAILABILITY

All data generated during this study are included in this published article, its supplementary information files and deposited in GenBank (PP565243–PP565334, PP573309–PP573503 & SRR28509296–SRR28509312).

REFERENCES

- Ahmadi M, Hemami M, Kaboli M *et al.* MaxEnt brings comparable results when the input data are being completed; Model parameterization of four species distribution models. *Ecology and Evolution* 2023; **13**:e9827. <https://doi.org/10.1002/ece3.9827>
- Aksenova O, Vinarski M, Bolotov I *et al.* Two *Radix* spp. (Gastropoda: Lymnaeidae) endemic to thermal springs around Lake Baikal represent ecotypes of the widespread *Radix auricularia*. *Journal of Zoological Systematics and Evolutionary Research* 2017; **55**:298–309. <https://doi.org/10.1111/jzs.12174>
- Angelis K, Dos Reis M. The impact of ancestral population size and incomplete lineage sorting on Bayesian estimation of species divergence times. *Current Zoology* 2015; **61**:874–85. <https://doi.org/10.1093/czoolo/61.5.874>
- Armbruster GFJ, Van Moorsel CHM, Gittenberger E. Conserved sequence patterns in the non-coding ribosomal ITS-1 of distantly related snail taxa. *Journal of Molluscan Studies* 2000; **66**:570–3.
- Bespalaya YV, Kropotin AV, Kondakov AV *et al.* A taxonomic reassessment of native and invasive species of *Corbicula* clams (Bivalvia: Cyrenidae) from the Russian Far East and Korea. *Zoological Journal of the Linnean Society* 2023; **197**:104–26. <https://doi.org/10.1093/zoolinnean/zlac078>
- Boettger O. Zwei neue Landschnecken aus dem Tertiärkalk von Hochheim. *Nachrichtsblatt der Deutschen Malakozoologischen Gesellschaft* 1903; **35**:182–4.
- Bouchet P, Rocroi JP, Hausdorf B *et al.* Revised classification, nomenclator and typification of gastropod and monoplacophoran families. *Malacologia* 2017; **61**:1–526. <https://doi.org/10.4002/040.061.0201>
- Brozzo A, Harl J, De Mattia W *et al.* Molecular phylogeny and trait evolution of Madeiran land snails: radiation of the Geomitridae (Stylommatophora: Helicoidea: Geomitridae). *Cladistics* 2020; **36**:594–616. <https://doi.org/10.1111/cla.12440>
- Capella-Gutiérrez S, Silla-Martínez JM, Gabaldón T. trimAl: a tool for automated alignment trimming in large-scale phylogenetic analyses. *Bioinformatics* 2009; **25**:1972–3.
- Cheddadi R, Vendramin GG, Litt T *et al.* Imprints of glacial refugia in the modern genetic diversity of *Pinus sylvestris*. *Global Ecology and Biogeography* 2006; **15**:271–82. <https://doi.org/10.1111/j.1466-8238.2006.00226.x>
- Chifman J, Kubatko L. Quartet inference from SNP data under the coalescent model. *Bioinformatics* 2014; **30**:3317–24. <https://doi.org/10.1093/bioinformatics/btu530>

- De Winter AJT, van Leeuwen S, Hovestadt A. A new species of *Glyphyalus* (Gastropoda, Pulmonata, Oxychilidae) from the Dutch Caribbean island of St. Eustatius. *Basteria* 2016;**80**:39–46.
- Dussex N, Wegmann D, Robertson BC. Postglacial expansion and not human influence best explains the population structure in the endangered kea (*Nestor notabilis*). *Molecular Ecology* 2014;**23**:2193–209. <https://doi.org/10.1111/mec.12729>
- Eaton DAR, Overcast I. Interactive assembly and analysis of RADseq datasets. *Bioinformatics* 2020;**36**:2592–4.
- Edgar RC. MUSCLE: multiple sequence alignment with high accuracy and high throughput. *Nucleic Acids Research* 2004;**32**:1792–7. <https://doi.org/10.1093/nar/gkh340>
- Ehlers J, Gibbard PL, Hughes PD (eds). *Quaternary Glaciations - Extent and Chronology: A Closer Look*. Amsterdam: Elsevier, 2011.
- Fick SE, Hijmans RJ. WorldClim 2: new 1-km spatial resolution climate surfaces for global land areas. *International Journal of Climatology* 2017;**37**:4302–15. <https://doi.org/10.1002/joc.5086>
- Flouri T, Huang J, Jiao X *et al.* Bayesian phylogenetic inference using relaxed-clocks and the multispecies coalescent. *Molecular Biology and Evolution* 2022;**39**:msac161. <https://doi.org/10.1093/molbev/msac161>
- Flouri T, Jiao X, Rannala B *et al.* Species tree inference with BPP using genomic sequences and the multispecies coalescent. *Molecular Biology and Evolution* 2018;**35**:2585–93. <https://doi.org/10.1093/molbev/msy147>
- Gadagkar SR, Rosenberg MS, Kumar S. Inferring species phylogenies from multiple genes: concatenated sequence tree versus consensus gene tree. *Journal of Experimental Zoology. Part B. Molecular and Developmental Evolution* 2005;**304B**:64–74. <https://doi.org/10.1002/jez.b.21026>
- Gent PR, Danabasoglu G, Donner LJ *et al.* The community climate system model version 4. *Journal of Climate* 2011;**24**:4973–91.
- Graf DL. Palearctic freshwater mussel (Mollusca: Bivalvia: Unionoidea) diversity and the comparative method as a species concept. *Proceedings of the Academy of Natural Sciences of Philadelphia* 2007;**156**:71–88. [https://doi.org/10.1635/0097-3157\(2007\)156\[71:pffmbu\]2.0.co;2](https://doi.org/10.1635/0097-3157(2007)156[71:pffmbu]2.0.co;2)
- Haponski AE, Lee T, Foighil DO. Moorean and Tahitian *Partula* tree snail survival after a mass extinction: new genomic insights using museum specimens. *Molecular Phylogenetics and Evolution* 2017;**106**:151–7.
- Harl J, Haring E, Páll-Gergely B. Hybridization and recurrent evolution of left-right reversal in the land snail genus *Schileykula* (Orculidae, Pulmonata). *Journal of Zoological Systematics and Evolutionary Research* 2020;**58**:633–47.
- Haase M, Meng S, Horskák M. Tracking parallel adaptation of shell morphology through geological times in the land snail genus *Pupilla* (Gastropoda: Stylommatophora: Pupillidae). *Zoological Journal of the Linnean Society* 2021;**191**:720–47.
- Hausdorf B. Phylogeny of the Limacoidea *sensu lato* (Gastropoda: Stylommatophora). *Journal of Molluscan Studies* 1998;**64**:35–66. <https://doi.org/10.1093/mollus/64.1.35>
- Hausdorf B, Neiber MT. Phylogeny and evolution of the land snail tribe Clausiliini (Gastropoda: Clausiliidae). *Molecular Phylogenetics and Evolution* 2022;**175**:107562. <https://doi.org/10.1016/j.ympev.2022.107562>
- Hayase Y, Kimura S, Kawabe K *et al.* A study on the non-marine molluscan fauna of a coastal area in northern Miyagi Prefecture, Japan after the 2011 Great East Japan Earthquake and Tsunami. *Chiribotan* 2016;**46**:2–62.
- Hijmans RJ, Cameron SE, Parra JL *et al.* Very high resolution interpolated climate surfaces for global land areas. *International Journal of Climatology* 2005;**25**:1965–78. <https://doi.org/10.1002/joc.1276>
- Hijmans, RJ, Phillips S, Leathwick J, Elith J. *Dismo: species distribution modeling. R package version 1.3.9*. 2021. <https://CRAN.R-project.org/package=dismo>
- Hirano T, Kameda Y, Saito T *et al.* Divergence before and after the isolation of islands: phylogeography of the *Bradybaena* land snails on the Ryukyu Islands of Japan. *Journal of Biogeography* 2019;**46**:1197–213. <https://doi.org/10.1111/jbi.13575>
- Hirano T, Saito T, Ito S *et al.* Phylogenomic analyses reveal incongruences between divergence times and fossil records of freshwater snails in East Asia. *Molecular Phylogenetics and Evolution* 2023;**182**:107728. <https://doi.org/10.1016/j.ympev.2023.107728>
- Hoang DT, Chernomor O, Von Haeseler A *et al.* UFBoot2: improving the ultrafast bootstrap approximation. *Molecular Biology and Evolution* 2018;**35**:518–22. <https://doi.org/10.1093/molbev/msx281>
- Hope AG, Speer KA, Demboski JR *et al.* A climate for speciation: rapid spatial diversification within the *Sorex cinereus* complex of shrews. *Molecular Phylogenetics and Evolution* 2012;**64**:671–84. <https://doi.org/10.1016/j.ympev.2012.05.021>
- Horskák M, Juříčková L, Pícká J. *Molluscs of the Czech and Slovak Republics*. Zlín: Kabourek, 2013.
- Horskáková V, Hájek M, Hájková P *et al.* Principal factors controlling the species richness of European fens differ between habitat specialists and matrix-derived species. *Diversity and Distributions* 2018;**24**:742–54. <https://doi.org/10.1111/ddi.12718>
- Horskáková V, Nekola JC, Horskák M. When is a 'cryptic' species not a cryptic species: a consideration from the Holarctic micro-landsnail genus *Euconulus* (Gastropoda: Stylommatophora). *Molecular Phylogenetics and Evolution* 2019;**132**:307–20. <https://doi.org/10.1016/j.ympev.2018.12.004>
- Horskáková V, Nekola JC, Horskák M. Integrative taxonomic consideration of the Holarctic *Euconulus fulvus* group of land snails (Gastropoda, Stylommatophora). *Systematics and Biodiversity* 2020;**18**:142–60. <https://doi.org/10.1080/14772000.2020.1725172>
- Hubricht L. The distributions of the native land mollusks of the eastern United States. *Fieldiana New Series* 1985;**24**:1–191.
- Hwang C, Ger M, Wu S. Within-island diversification in the land snail genus *Formosana* (Gastropoda, Clausiliidae) in Taiwan. *Zoologica Scripta* 2022;**51**:562–88. <https://doi.org/10.1111/zsc.12557>
- Jungclaus J, Giorgetta M, Reick C, *et al.* CMIP5 simulations of the Max Planck Institute for Meteorology (MPI-M) based on the MPI-ESM-P model: the *Igm* experiment, served by ESGF. World Data Center for Climate (WDCC) at DKRZ, 2011. <https://doi.org/10.1594/WDCC/CMIP5.MXEP1g>
- Kaky E, Nolan V, Alatawi A *et al.* A comparison between Ensemble and MaxEnt species distribution modelling approaches for conservation: a case study with Egyptian medicinal plants. *Ecological Informatics* 2020;**60**:101150. <https://doi.org/10.1016/j.ecoinf.2020.101150>
- Kalyaanamoorthy S, Minh BQ, Wong TKF *et al.* ModelFinder: fast model selection for accurate phylogenetic estimates. *Nature Methods* 2017;**14**:587–9. <https://doi.org/10.1038/nmeth.4285>
- Kass JM, Muscarella R, Galante PJ *et al.* ENMeval 2.0: redesigned for customizable and reproducible modeling of species' niches and distributions. *Methods in Ecology and Evolution* 2021;**12**:1602–8. <https://doi.org/10.1111/2041-210x.13628>
- Kerney MP. *Atlas of the land and freshwater molluscs of Britain and Ireland*. Colchester, UK: Harley Books, 1999.
- Kleckova I, Cesanek M, Fric Z *et al.* Diversification of the cold-adapted butterfly genus *Oeneis* related to Holarctic biogeography and climatic niche shifts. *Molecular Phylogenetics and Evolution* 2015;**92**:255–65. <https://doi.org/10.1016/j.ympev.2015.06.012>
- Köhler F, Criscione F. Plio-Pleistocene out-of-Australia dispersal in a camaenid land snail. *Journal of Biogeography* 2014;**40**:1971–82.
- Korniushin AV. Review of the studies on freshwater mollusc systematics carried out by the Russian taxonomic school. *Malacological Review Supplement* 1998;**7**:65–82.
- Kumar S, Stecher G, Tamura K. MEGA7: molecular evolutionary genetics analysis version 7.0 for bigger datasets. *Molecular Biology and Evolution* 2016;**33**:1870–4. <https://doi.org/10.1093/molbev/msw054>
- Lanfear R, Frandsen PB, Wright AM *et al.* PartitionFinder 2: new methods for selecting partitioned models of evolution for molecular and morphological phylogenetic analyses. *Molecular Biology and Evolution* 2017;**34**:772–3. <https://doi.org/10.1093/molbev/msw260>
- Lobo JM, Jiménez-Valverde A, Real R. AUC: a misleading measure of the performance of predictive distribution models. *Global Ecology and Biogeography* 2008;**17**:145–51.

- Merow C, Smith MJ, Silander JA. A practical guide to MaxEnt for modeling species' distributions: what it does, and why inputs and settings matter. *Ecography* 2013;**36**:1058–69. <https://doi.org/10.1111/j.1600-0587.2013.07872.x>
- Minh BQ, Schmidt HA, Chernomor O *et al.* IQ-TREE 2: new models and efficient methods for phylogenetic inference in the genomic era. *Molecular Biology and Evolution* 2020;**37**:1530–4. <https://doi.org/10.1093/molbev/msaa015>
- MolluscaBase. MolluscaBase. <https://www.molluscabase.org>. 2024. <https://doi.org/10.14284/448>
- Morii Y, Yokoyama J, Kawata M *et al.* Evidence of introgressive hybridization between the morphologically divergent land snails *Ainohelix* and *Ezohelix*: introgressive hybridization. *Biological Journal of the Linnean Society* 2015;**115**:77–95. <https://doi.org/10.1111/bij.12466>
- Murray-Wallace CV. Barystatic sea-level changes—glacial–interglacial cycles. In: *Reference Module in Earth Systems and Environmental Sciences*. Elsevier, 2023. <https://doi.org/10.1016/B978-0-323-99931-1.00049-0>
- Neiber MT, Chueca LJ, Caro A *et al.* Incorporating palaeogeography into ancestral area estimation can explain the disjunct distribution of land snails in Macaronesia and the Balearic Islands (Helicidae: Allognathini). *Molecular Phylogenetics and Evolution* 2021;**162**:107196. <https://doi.org/10.1016/j.ympev.2021.107196>
- Neiber MT, Walther F, Kijashko PV *et al.* The role of Anatolia in the origin of the Caucasus biodiversity hotspot illustrated by land snails in the genus *Oxychilus*. *Cladistics* 2022;**38**:83–102. <https://doi.org/10.1111/cla.12479>
- Nekola JC. Terrestrial gastropod fauna of northeastern Wisconsin and the Southern Upper Peninsula of Michigan. *American Malacological Bulletin* 2004;**18**:21–44.
- Nekola JC, Chiba S, Coles BF *et al.* A phylogenetic overview of the genus *Vertigo* O. F. Müller, 1773 (Gastropoda: Pulmonata: Pupillidae: Vertigininae). *Malacologia* 2018;**62**:21–161.
- Nekola JC, Coles BF, Horsák M. Species assignment in *Pupilla* (Gastropoda: Pulmonata: Pupillidae): integration of DNA-sequence data and conchology. *Journal of Molluscan Studies* 2015;**81**:196–216. <https://doi.org/10.1093/molstud/eyu083>
- Nekola JC, Divišek J, Horsák M. The nature of dispersal barriers and their impact on regional species pool richness and turnover. *Global Ecology and Biogeography* 2022a;**31**:1470–500. <https://doi.org/10.1111/geb.13517>
- Nekola JC, Horsák M. The impact of empirically unverified taxonomic concepts on ecological assemblage patterns across multiple spatial scales. *Ecography* 2022;**2022**:e06063.
- Nekola JC, Nováková M, Horsák M *et al.* ELAV Intron 8: a single-copy sequence marker for shallow to deep phylogeny in *Eupulmonata* Hasprunar & Huber, 1990 and *Hygrophila* Férussac, 1822 (Gastropoda: Mollusca). *Organisms Diversity & Evolution* 2022b;**23**:621–9. <https://doi.org/10.1007/s13127-022-00587-3>
- Nekola JC, White PS. The distance decay of similarity in biogeography and ecology. *Journal of Biogeography* 1999;**26**:867–78. <https://doi.org/10.1046/j.1365-2699.1999.00305.x>
- Perkins-Taylor IE, Frey JK. Predicting the distribution of a rare chipmunk (*Neotamias quadrivittatus oscuraensis*): comparing MaxEnt and occupancy models. *Journal of Mammalogy* 2020;**101**:1035–48. <https://doi.org/10.1093/jmammal/gyaa057>
- Peterson BK, Weber JN, Kay EH *et al.* Double digest RADseq: an inexpensive method for *de novo* SNP discovery and genotyping in model and non-model species. *PLoS One* 2012;**7**:e37135. <https://doi.org/10.1371/journal.pone.0037135>
- Phillips SJ, Anderson RP, Dudík M *et al.* Opening the black box: an open-source release of Maxent. *Ecography* 2017;**40**:887–93. <https://doi.org/10.1111/ecog.03049>
- Phillips SJ, Anderson RP, Schapire RE. Maximum entropy modeling of species geographic distributions. *Ecological Modelling* 2006;**190**:231–59. <https://doi.org/10.1016/j.ecolmodel.2005.03.026>
- Pilsbry HA. *Land Mollusca of North America (North of Mexico)*. Monograph no. 3. Philadelphia, PA: Academy of Natural Sciences of Philadelphia, 1948.
- QGIS Development Team. *QGIS Geographic Information System Version 3.16. Open Source Geospatial Foundation Project*. <http://qgis.osgeo.org>, 2020 (12 Dec 2020, date last accessed).
- R Core Team. *R: A Language and Environment for Statistical Computing*. Vienna, Austria: R Foundation for Statistical Computing. <https://www.R-project.org/>, 2022.
- Rambaut A, Drummond AJ, Xie D *et al.* Posterior summarization in Bayesian phylogenetics using Tracer 1.7. *Systematic Biology* 2018;**67**:901–4. <https://doi.org/10.1093/sysbio/syy032>
- Rannala B, Yang Z. Bayes estimation of species divergence times and ancestral population sizes using DNA sequences from multiple loci. *Genetics* 2003;**164**:1645–56. <https://doi.org/10.1093/genetics/164.4.1645>
- Reaz R, Bayzid MS, Rahman MS. Accurate phylogenetic tree reconstruction from quartets: a heuristic approach. *PLoS One* 2014;**9**:e104008.
- Ricklefs RE, Schluter D. Species diversity: regional and historical influences. In: Ricklefs RE, Schluter D, (ed). *Species Diversity in Ecological Communities*. Chicago, IL: University of Chicago Press, 1993, 350–63.
- Roberts DR, Hamann A. Glacial refugia and modern genetic diversity of 22 western North American tree species. *Proceedings Biological Sciences* 2015;**282**:20142903. <https://doi.org/10.1098/rspb.2014.2903>
- Ronquist F, Huelsenbeck JP. MrBayes 3: Bayesian phylogenetic inference under mixed models. *Bioinformatics* 2003;**19**:1572–4. <https://doi.org/10.1093/bioinformatics/btg180>
- Sano I, Saito T, Ito S *et al.* Resolving species-level diversity of *Beringiana* and *Sinanodontia* mussels (Bivalvia: Unioniidae) in the Japanese archipelago using genome-wide data. *Molecular Phylogenetics and Evolution* 2022;**175**:107563. <https://doi.org/10.1016/j.ympev.2022.107563>
- Schär S, Talavera G, Espadaler X *et al.* Do Holarctic ant species exist? Trans-Beringian dispersal and homoplasy in the Formicidae. *Journal of Biogeography* 2018;**45**:1917–28. <https://doi.org/10.1111/jbi.13380>
- Schlickum WR, Strauch F. Zur Systematik westeuropäischer neogener Zonitidae. *Archiv für Molluskenkunde* 1975;**106**:39–45.
- Stecher G, Tamura K, Kumar S. Molecular evolutionary genetics analysis (MEGA) for macOS. *Molecular Biology and Evolution* 2020;**37**:1237–9. <https://doi.org/10.1093/molbev/msz312>
- Swofford D. *PAUP* Phylogenetic analysis using parsimony (* and other methods) v.4.0a168*. Sunderland, MA: Sinauer Associates, 2002.
- Sysoev A, Schileyko A. *Land Snails and Slugs of Russia and Adjacent Countries*. Sofia: Pensoft, 2009.
- Tamura K, Battistuzzi FU, Billings-Ross P *et al.* Estimating divergence times in large molecular phylogenies. *Proceedings of the National Academy of Sciences of the United States of America* 2012;**109**:19333–8. <https://doi.org/10.1073/pnas.1213199109>
- Tamura K, Tao Q, Kumar S. Theoretical foundation of the RelTime method for estimating divergence times from variable evolutionary rates. *Molecular Biology and Evolution* 2018;**35**:1770–82. <https://doi.org/10.1093/molbev/msy044>
- Tao Q, Tamura K, Mello B *et al.* Reliable confidence intervals for RelTime estimates of evolutionary divergence times. *Molecular Biology and Evolution* 2020;**37**:280–90. <https://doi.org/10.1093/molbev/msz236>
- Toews DPL, Irwin DE. Cryptic speciation in a Holarctic passerine revealed by genetic and bioacoustic analyses. *Molecular Ecology* 2008;**17**:2691–705. <https://doi.org/10.1111/j.1365-294X.2008.03769.x>
- Villesen PF. FaBox: an online toolbox for fasta sequences. *Molecular Ecology Notes* 2009;**7**:965–8.
- Vinarski MV. The species question in freshwater malacology: from Linnaeus to the present day. *Folia Malacologica* 2018;**26**:39–52. <https://doi.org/10.12657/folmal.026.005>
- Vinarski MV, Kramarenko SS. How does the discrepancies among taxonomists affect macroecological patterns? A case study of freshwater snails of Western Siberia. *Biodiversity and Conservation* 2015;**24**:2079–91. <https://doi.org/10.1007/s10531-015-0934-4>
- Waldén, H. *Svensk Landmolluskatlas*. Stenungsund: Naturcentrum AB, 2007.
- Warren DL, Seifert SN. Ecological niche modeling in Maxent: the importance of model complexity and the performance of model selection criteria. *Ecological Applications* 2011;**21**:335–42. <https://doi.org/10.1890/10.1171.1>

- Wascher M, Kubatko L. Consistency of SVDQuartets and maximum likelihood for coalescent-based species tree estimation. *Systematic Biology* 2021;**70**:33–48. <https://doi.org/10.1093/sysbio/syaa039>
- Watanabe S, Hajima T, Sudo K *et al.* MIROC-ESM 2010: model description and basic results of CMIP5-20c3m experiments. *Geoscientific Model Development* 2011;**4**:845–72. <https://doi.org/10.5194/gmd-4-845-2011>
- Weir JT, Schluter D. Ice sheets promote speciation in boreal birds. *Proceedings Biological Sciences* 2004;**271**:1881–7. <https://doi.org/10.1098/rspb.2004.2803>
- Weir JT, Haddrath O, Robertson HA *et al.* Explosive ice age diversification of kiwi. *Proceedings of the National Academy of Sciences of the United States of America* 2016;**113**:E5580–7. <https://doi.org/10.1073/pnas.1603795113>
- Welter-Schultes FW. *European Non-Marine Molluscs, a Guide for Species Identification*. Göttingen: Planet Poster Editions, 2012.